

Digital Darkfield Analysis of Nanoparticle Defects

P. Fraundorf^{* **}, J. Liu^{* **}, and E. Mandell^{*}

^{*} Department of Physics and Astronomy, University of Missouri-St. Louis, One University Blvd, St. Louis, MO 63121

^{**} Center for Molecular Electronics, University of Missouri-St. Louis, One University Blvd, St. Louis, MO 63121

Microscopists have done combined space and frequency decompositions optically since long before coining of the word “wavelet” [1], under the name “darkfield imaging” [2]. Now integrative views of lattice information in digital images yield new challenges for mathematical harmonic analysis [3]. Such challenges are illustrated by a series of notes [4-7] on the uses and shortcomings of “weakly convergent” Fourier transform window techniques. Here, we show how robust (if pedestrian) digital darkfield techniques help to characterize: (i) an Antimony-doped Tin Oxide nanoparticle screw dislocation, and (ii) twinning and strain in a gold decahedral twin.

Each row in the figures at right contains a power spectrum used to select a reference “g-vector” of interest, followed by a complex-color map of darkfield amplitude (intensity) and phase (hue) with respect to that g-vector. The remaining two columns use coordinate-color to show isotropic strain (red is compressed, cyan is expanded) and shear strain (chartreuse is clockwise and indigo is counter clockwise) with respect to that reference. Each pixel in these is a fractional strain measurement.

The (110) planes in the ATO grain of Fig. 1 (top row) show a 180 degree phase-lag between the top and bottom half of the crystal in the darkfield, in spite of the spacing uniformity (seen in both the phase beats of the complex darkfield image, and comparable top/bottom intensities in the strain maps). The other reflections (e.g. rows 2 and 3) do not share this phase lag, indicating that the (110) planes indeed form a “spiral staircase” running from left to right that moves up by $\frac{1}{2} g_{110} = 0.167\text{nm}$ for each half-turn. Quantitative information on the rate of strain relaxation around this dislocation [cf. 8] is available in this image as well.

Digital darkfield analysis of the gold decahedral grain near the 5-fold zone in Fig. 2 shows single-slice wedges for (200) and (220) reflections, in place of the “bowties” seen for icosahedral twins [7], and double-slice wedges for (111) reflections in place of icotwin “butterflies”. Notice also the absence of a (111) discontinuity bisecting the double-slice wedges. This puts picometer-scale limits on the bulk-driven build up of strain between sub-domains in this tiny particle.

References

- [1] P. Goupillaud et al, *Geoexploration* **23** (1984) 85.
- [2] cf. P. Hirsch et al, “Electron Microscopy of Thin Crystals” (Krieger, NY, 1977).
- [3] P. Fraundorf, “Digital Darkfield Decompositions” (2004) arXiv:cond-mat/**0403017**.
- [4] P. Fraundorf and G. K. Fraundorf, *Proc. 47th Ann. EMSA Meeting* (1989) 122.
- [5] P. Fraundorf and Lu Fei, *Microsc. Microanal.* **10** (Suppl. 2) (2004) 300.
- [6] M. Rose and P. Fraundorf, *Microsc. Microanal.* **12** (Suppl. 2) (2006) 1008.
- [7] P. Fraundorf, J. Wang, E. Mandell and M. Rose, *ibid.* (2006) 1010.
- [8] C. L. Johnson, M. J. Hÿtch and P. R. Buseck, *Amer. Min.* **89** (2004) 1374.

Figure 1:
 HREM image of an
 antimony-doped SnO₂
 nanoparticle, viewed down
 the cassiterite <111> zone.
 The figure layout is
 discussed in the text. The
 first-row darkfield shows a
 screw dislocation running
 from left to right along (110).

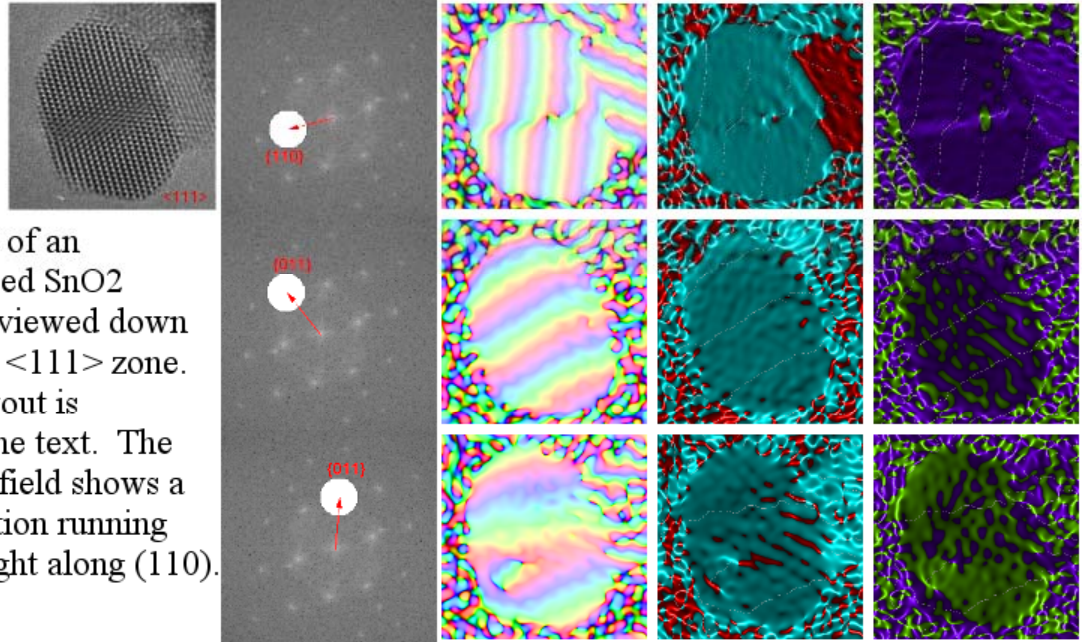


Figure 2:
 HREM image of a
 decahedral gold crystal
 down the 5-fold
 symmetry axis.
 Sub-domains show
 up in digital darkfield
 as single and double
 pie-slices. The latter
 allow one to map
 projected strain at
 (111) boundaries. The
 3rd and 4th rows show
 the effect of aperture
 size.

